2016 24th International Lightning Detection Conference & 6th International Lightning Meteorology Conference
18 - 21 April | San Diego, California, USA

Characteristics of the Distribution, Initiation, Motion, and Evolution of the Thunderstorms over the Yangtze River Delta Region

DAI Jianhua*, TAO Lan, and SUN Min
Shanghai Central Meteorological Observatory
China Meteorological Administration
Shanghai, China
* djhnn@sina.com

***Abstract*—Using the WSR-88D Doppler Weather radar and the Vaisala lightning detection data, some characteristics (the spatiotemporal distributions and motion features) of thunderstorms over the Yangtze River Delta (YRD) region are investigated. Local storms tend to be cluster over cities, isolated mountains or hills, and water-land borders. Storm intensifying centers are found about 10-30 km downwind of the city centers, while the medium-path storms also show a downwind effect with a distance of from medium-sized cities and centers of larger cities about 10 km farther than those of local storms. In Shanghai, sea-breeze front is found to be more important for local thunderstorm initiation and development than the urban heat island effect. Vertical structure of storm cell and lightning activity during the evolutionary stages of several types of thunderstorms are also analyzed, and a basic conceptual model of thunderstorm evolution is given. The mechanisms of thunderstorm initiation and evolution are discussed for the YRD region.**

Keywords*—thunderstorm; lightning; initiation and evolution; urban heat island; sea-breeze front

I. INTRODUCTION

The Yangtze River Delta (YRD) (Fig.1), including Shanghai City and the adjacent parts of Zhejiang Province and Jiangsu Province, is washed by the East China Sea to the east and Hangzhou Bay to the south. North of the delta the Yangtze River pours into the East China Sea. The YRD also occupies a central location along China's coastline. Except for a few hills lying in the southwest corner, most parts of the Shanghai area are flat and belong to the alluvial plain of the Yangtze River Delta. The YRD in the South and west of Zhejiang has many mountains and hills, like Tianmu Mountain, Huiji Mountain, Siming Mountain, and Tiantai Mountain. In the south Jiangsu Province and Zhejiang Province, there are many medium-sized cities, such as Changzhou, Wuxi, Suzhou, Hangzhou, Shaoxing, and Ningbo. Dotted with many rivers and lakes, the YRD is known for its rich water resources.

Topography, surface features and the urban heat island all play important roles in YRD's weather. In the YRD, for example like Shanghai, receives an average annual rainfall of 1,200 mm; nearly 60% of the precipitation comes during the April-September warm season. During July and September, thunderstorms with lightning strikes, heavy rain, hail and damaging winds (squalls) become frequent. On average there are 15 rainy days and 8 thunderstorm days per month in the warm seasons.

Using the WSR-88D Doppler Weather radar and the Vaisala lightning detection data, some characteristics (the spatiotemporal distributions and motion features) of thunderstorms over the Yangtze River Delta region are investigated.

Fig. 1. Topography of the Yangtze River Delta (http://maps.baidu.com).

Supported by National Natural Science Foundation of China (41175050) and Meteorological Research Program of China (GYHY201006002)

II. Data

A. Radar Derived Products

The Weather Surveillance Radar-1988 Doppler (WSR-88D)'s Storm Cell Identification and Tracking (SCIT) product includes some structural information about a cell, such as echo top (ET), Vertically Integrated Liquid (VIL), height of maximum reflectivity (MRHgt) [Johnson et al., 1998]. SCIT has been used to identify and track storm cells with a threshold of maximum reflectivity about 35 dBZ. The Shanghai Nanhui WSR-88D SCIT products during 2004 to 2012 are used to selected thunderstorm cases for the Yangtze River Delta based on the criterion that thunderstorm's VIL reaches 15 kg/m^2 at least once in a life cycle of cell.

Cell density of thunderstorm (*CellDen*, in 100 $cell\cdot month^{-1}\cdot km^{-2}$) was calculated by the unit time (month) and per unit area (100km^2). Each cell will be counted once each 6 min. *CellDen* is defined as:

$$CellDen = \frac{Cells}{Area \cdot Time} \tag{1}$$

Where, *Cells* is the number of thunderstorm cells counted for the study area.

Vertically Integrated Liquid (VIL) can provide information about the vertical development (top height and intensity) of a thunderstorm [Green and Clark, 1972]. Therefore, it can be used as an important index for the diagnosis of severe weather.

In order to describe the evolution of thunderstorm, VIL difference between two adjacent times is calculated to get the intensity change of a cell.

$$\Delta VIL_t = VIL_t - VIL_{t-1} \tag{2}$$

where, VIL_t and VIL_{t-1} for time t and time t-1.

B. Lightning Data

Lightning observations have been used for thunderstorm climtology and storm severity study for many years [Macgorman and Burgess, 1994; Reap and MacGroman, 1989; Williams et al., 1999; Dai et al., 2005]. In this study, the Shanghai Vaisala's total lightning localization system provides total lightning data from 2004-2012. The density of Could-to-Ground (CG) lightning flash - *CGDen* ($fl\cdot yr^{-1}\cdot km^{-2}$) is also calculated using the Vaisala lightning detection network of Shanghai.

C. Automated Weather Station Temperature Analysis

In order to reveal the meso-scale surface temperature distribution, 12:00 BJT (BeiJing time) automated weather station (AWS) temperature data over the YRD are averaged. For avoiding the mountain influence on temperature distribution and quality control, only those sites with an altitude below 120 m are used.

Fig. 2 shows 12:00BJT averaged temperature distribution during July and August for the years of 2009 to 2012. A clear urban heat island (UHI) of Shanghai can be found in the metropolitan area of Shanghai and Minhang District and Songjiang District [Shu et al., 2000; Zhang et al., 2009]. As a result of water-land effect, surface temperature rapidly changes at the northern parts of Baoshan District and Pudong District along the Yangtze River. Sanders [1999] defined a potential temperature gradient classification method for nonfrontal baroclinic zones (moderate intensity for 8 ºC /220km, strong to 8 ºC /110km). Due to most of local mid-summer thunderstorms show strong correlation with the UHI effect, sea-breeze fronts, and some hills in the YRD [Dai et al, 2005], a revised temperature gradient classification method for analyzing mesoscale phenomena is defined as: 1) moderate intensity for 2-3 ºC /12km (1-2 ºC /12km for long-term average value), and 2) strong temperature gradient for 3-6 ºC /12km (2-3 ºC /12km). Blue dots in Fig. 3 cover the similar nonfrontal baroclinic zones that temperature gradient is over 1 ºC /12km at 12:00 BJT for the mid-summer (July and August).

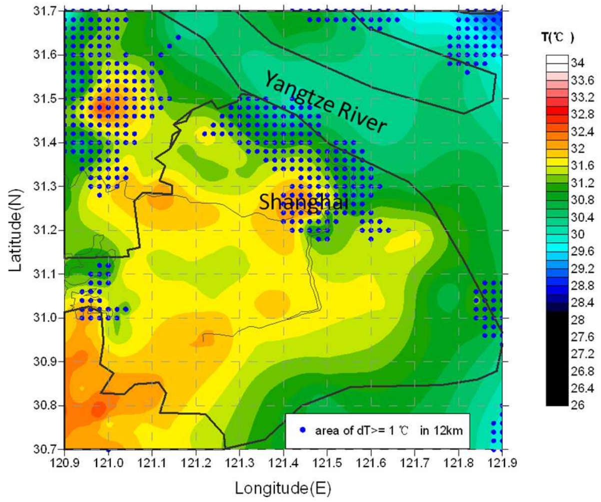

Fig. 2. Mean surface temperature (shaded) and zones with temperature gradient over 1 ºC /12 km (blue dots) at 12:00 BJT of automated weather stations in the Shanghai area in July and August of the years from 2009 to 2012.

III. Thunderstorm Statistics

A. Classification of Thunderstorms

Thunderstorms are classified based on synoptic condition and their intensity, cell moving distance, and lifecycle duration.

a) Synoptic Condition

According to the Yangtze River Delta's climatology [Dai et al., 2005], four types of thunderstorms are classified by their influence systems and/or synoptic condition: 1) during the Meiyu season (monsoon season); 2) tropical systems – tropical cyclone and easterly waves; 3) mid-summer period in July and August excluding 1) and 2); 4) others periods excluding 1) to 3) from April to September.

Meiyu seasons of the YRD are usually about 20 days between the late June and early July. The typical synoptic systems over the YRD relate to a persistent stationary front and sometime with cyclones. During the mid-summer, the YRD is occupied by the edge or body of the western North Pacific subtropical high, and local thunderstorms frequently are observed. Tropical systems, majorly tropical cyclones and/or sometimes easterly wavers, occasionally affect the YRD.

b) Thunderstorm Intensity

VIL is a good indicator of thunderstorm intensity and development [Ambum and Wolf, 1997; Greene and Clark, 1972]. Here, the strongest VIL (*VILmax*) in the history of lifecycle of a thunderstorm is used to categorize thunderstorms into three grades: grade I - *VILmax* at least 15 kg/m^2, grade II - *VILmax* at least 25 kg/m^2, and grade III - *VILmax* at least 40 kg/m^2.

c) Thunderstorm Moving Distance

Thunderstorms are also divided into three types based on their moving distance from the beginning to end in their lifecycle: local cells (0-30km), mid-distance moving cells (30-60km) and long distance moving cells (at least 60km).

d) Thunderstorm Lifecycle Duration

For finding characteristics of thunderstorm evolution, thunderstorms are categorized into 3 categories by the duration of lifecycle: Category I (48 - 72 minutes), Category II (78 - 102 minutes), and Category III (108 - 132 minutes). Category 0049 (III) are mainly the pulse or local thunderstorms (long-lived thunderstorms), and Category II are the mix of I and III.

B. *Thunderstorm Frequency*

Table I and Table II show thunderstorm frequency in Category I (lifecycle about 60 min) with a *VILmax* at least 15 kg/m^2 (Grade I) and 25 kg/m^2 (Grade II) in different synoptic conditions, respectively.

TABLE I. Warm Season (Apr. to Sep.) Thunderstorm (Maximum VIL≥15kg/m^2) frequency by synopitc type during 2004 -2012

Proportion (%)	Lifecycle Moving Distance (VIL≥15 kg/m^2)			
	Local (0-30km)	*Mid-Distance Moving (30-60km)*	*Long Distance Moving (at least 60km)*	*All*
Monsoon	74.2	21.0	4.8	28.2
Mid-summer	82.5	14.0	3.5	54.3
Tropical systems	38.5	27.7	33.8	3.6
Others	69.8	22.5	7.7	17.4
All	77.9	17.5	4.6	100.0

TABLE II. the same as Table I, except for those Thunderstorms(Maximum VIL≥25kg/m^2)

Proportion (%)	Lifecycle Moving Distance (VIL≥25 kg/m^2)			
	Local (0-30km)	*Mid-Distance Moving (30-60km)*	*Long Distance Moving (at least 60km)*	*All*
Monsoon	75.0	20.6	4.4	27.1
Mid-summer	84.9	13.0	2.1	58.3
Tropical systems	**58.6**	**21.8**	**19.6**	1.1
Others	72.2	21.2	6.6	14.5
All	80.4	16.3	3.3	100.0

During the warm season (Apr. to Sep.) of the years from 2004-2012 in the YRD, more thunderstorms occurred in mid-summer than other periods, and the monsoon season ranked second. Table I shows most of Grade-I thunderstorms with a *VILmax* at least 15kg/m^2 occurred in the mid-summer (54.3%) and the monsoon season (28.2%) or June to August. For the Grade-II thunderstorms with a *VILmax* at least 25kg/m^2, more (58.3%) were observed in the mid-summer, which shows more stronger thunderstorms occur in mid-summer and fewer in tropical systems and other periods. Least of thunderstorms both in Grade I and II were found in tropical systems because tropical systems less affected the YRD.

On the other hand, local storms frequently occurred in the YRD. For the moving distance of a thunderstorm from the beginning to end, most (77.9%) of Grade-I thunderstorms (with a *VILmax* at least 15kg/m^2) were local ones, while the mid-distance moving cells accounted for 17.5% and the long distance moving only 4.6%. The proportion of the local Grade-II thunderstorms slightly increased to 80.4%, and other tow types went down to 16.3% and 3.3%. In contrast, the longer distance moving Grade I cells' proportion in tropical systems ranked first, especially the long distance moving ones with a biggest proportion of 33.76%, much higher than other types of cells. For stronger (Grade II) long distance moving cells in tropical systems, local cells increased to 58.6% and long distance moving cells decreased to 19.6% from 33.8%. With stronger steering flows by tropical systems, thunderstorms tend to move faster than those in other synoptic conditions.

IV. SPATIAL DISTRIBUTIONS OF THUNDERSTORMS

Spatial distributions of thunderstorms over the YRD region were analyzed using the Vaisala CG lightning flash density and radar-derived thunderstorm cell density.

A. *Spatial Distribution of Lightning Density*

Fig. 3 shows the Vaisala CG lightning flash density *CGDen* （$fl{\cdot}yr^{-1}{\cdot}km^{-2}$） over the YRD in Jun. – Sep. of the years of 2008 to 2012. There are four high *CGDen* areas in the YRD. One of them is in Shanghai, including Jiading District, Baoshan District, the metropolitan area of Shanghai, and the northern Pudong New District. *CGDen* over these areas were over 30.0 $fl{\cdot}yr^{-1}{\cdot}km^{-2}$, and the maximum *CGDen* at the northern Shanghai Pudong New District reaching 52.0 $fl{\cdot}yr^{-1}{\cdot}km^{-2}$. Another two high CG density centers are located at Ningbo and the Tianmu Mountains.

In Fig. 4, the CG lightning flash density is overlaid with the surface "nonfrontal baroclinic" zones (blue dots) that has a surface temperature gradient at least 1 ºC /12 km in Shanghai. It is obvious that CG lightning is strongly correlated to the temperature gradient in the boundary layer. The stronger surface temperature gradient is, the more CG lightning flashes are observed. The low level thermal circulation caused by urban heat island and sea-breeze front may trigger and intensify vertical motion even if the synoptic forcing is absent. As a result, convection can be triggered by these updrafts if proper humidity condition and mid-level instability are available.

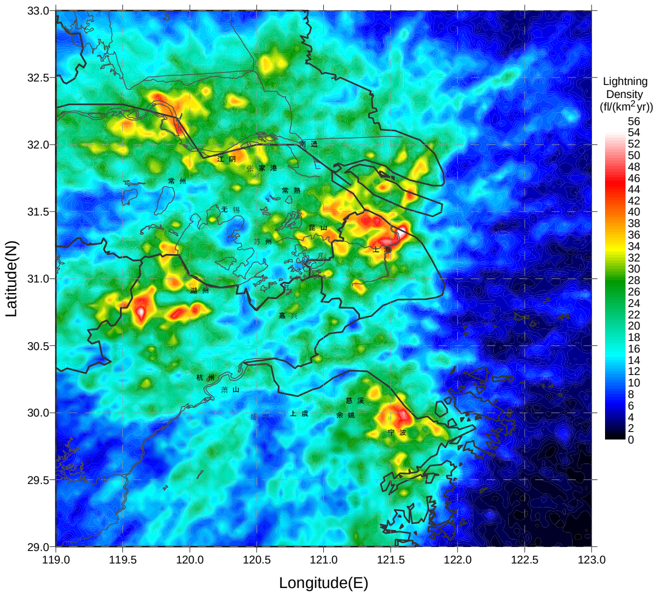

Fig. 3. Vaisala CG lightning flash density（*fl·yr*$^{-1}$*·km*$^{-2}$）over the Yangtze River Delta in Jun. – Sep. of the years of 2008 to 2012.

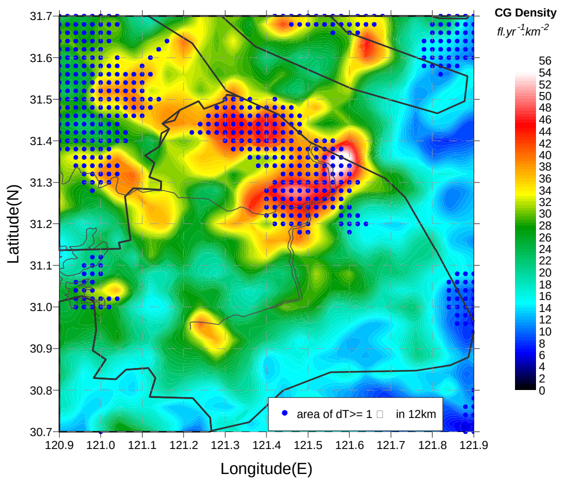

Fig. 4. CG lightning flash density lower and zones with surface temperature gradient over 1 ºC /12 km (blue dots) at 12:00 BJT for Shanghai in July and August of the years from 2009 to 2012.

B. *Spatial Distribution of Thunderstorm Cells*

Fig. 5 shows the cell density (*CellDen,* in *cell·month*$^{-1}$*·km*$^{-2}$) distribution of the YRD strong and long-lived thunderstorms (lifecycle at least 60min and maximum VIL at least 25 kg/m^2) during April to September 2004-2012. This type of thunderstorms cluster in some places with a *CellDen* at least 3.0 *cell·month*$^{-1}$*·km*$^{-2}$, and clearly relate to some large-sized to medium-sized cities, such as the Shanghai metropolitan and Shanghai's districts (the northern Minhang District and northern Pudong New District), some medium-sized cities (Changzhou, Wuxi, and Suzhou) close to the Lake Taihu in southern Jiangsu Province, some cities (Hangzhou, Shaoxing, Shangyu, and Ningbo, etc.) in Zhejiang Province, and mountains or/and hills. The mountains and hills are the Meishan close to Yixing at the border of Jiangsu Province and Zhejiang Province, the Tianmu Mountain northwest to Hangzhou city, and some mountains close to Ningbo, such as Siming Mountain, the north part of Tiantai Mountain, and the hill Dapeng (Cities, mountains, lakes, and rivers are shown in Fig.1) .

In conclusion, strong and long-lived thunderstorms over the YRD have good correlation with some local topography characteristics. The cell density centers are: 1) close to cities, especially those medium-sized cities; 2) over mountains or hills, especially those isolated mountains of hills; and 3) at the water-land borders. This implies solar radiation and difference of underlying surface features are major causes of thunderstorms initiation and development. If it meets two or three among these three conditions above at the same time, more probabilities of strong thunderstorms will initiate and develop. The area between the Yangcheng Lake and Kunshan has become the most active thunderstorm in eastern of south Jiangsu Province due to the urban heat island effect and the lake-land circulation. The most frequent thunderstorm occurrence in the YRD is located in Ningbo where is located along the Hangzhou Bay and close to the Siming Mountain and Tiantai Mountain. Proper conditions for convection development can be found in Ningbo, such as sea-land breeze circulation, valley wind circulation and/or terrain convergence, as well as the urban heat island effect.

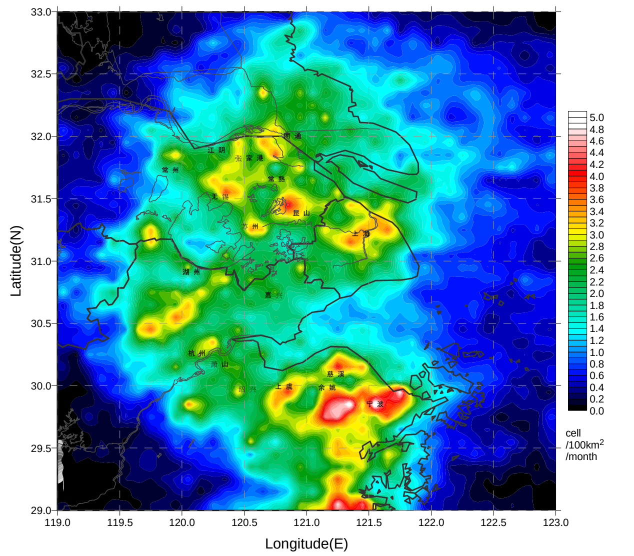

Fig. 5. Distribution density（in ×100 *cell·month*$^{-1}$*·km*$^{-2}$）of thunderstorm cells with a life cycle at least 60 min and the maximum VIL at least 25 kg/m^2 during the months from April to September in 2004 to 2012.

Since 80.4% of grade II (*VILmax* at least 25 kg/m^2) cells are local storms (moving distance during the lifecycle from the beginning to the end no more than 30km), Fig. 6 shows the similar cell density distribution patterns to those of all thunderstorms in Fig. 5.

Compared to local storms (Fig. 6), those medium distance moving thunderstorms (Fig. 7) tend to be close to some land-water borders. Only fewer high cell density centers relate to cities (Shanghai and Ningbo). It implies that the low level horizontal temperature gradient and corresponding wind shear or convergence zones along the land-water borders are suitable for maintenance and/or intensification of the mid-distance moving thunderstorms.

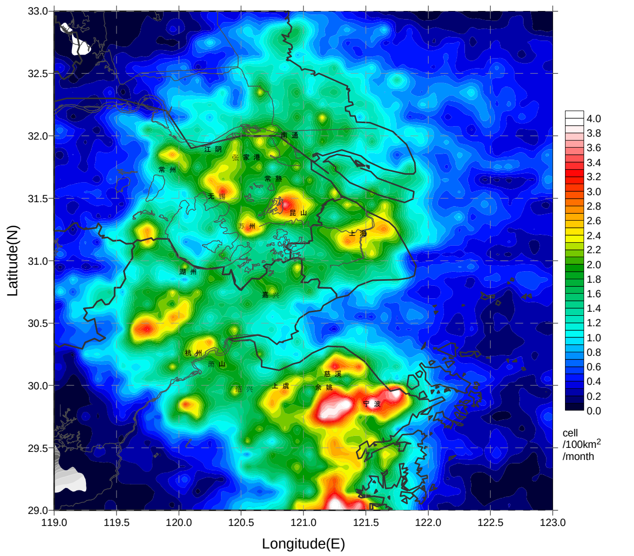

Fig. 6. the same as Fig. 5, but for those thunderstorms with a total path less than 30km.

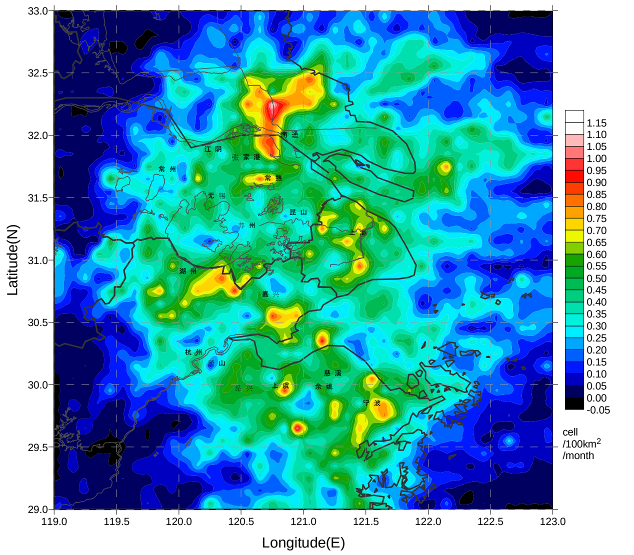

Fig. 7. the same as Fig. 5, but for those thunderstorms with a total path between 30 and 60 km.

Long path thunderstorms concentrate in several major corridors under certain synoptic situations. More right-moving storms are found under southwest flow, while a higher proportion of left-moving storms than right-moving are observed under northwest flow. Long life cycle and long path severe thunderstorms are found to have a tendency to move right.

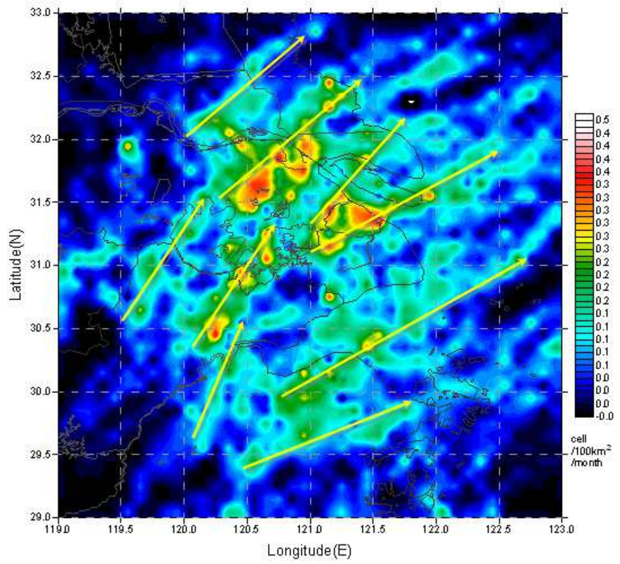

Fig. 8. the same as Fig. 5, but for those thunderstorms with a total path least than 60km (yellow arrows illustrate some mean motion patterns of the storms).

V. THUNDERSTORM INITIATION AND EVOLUTION

A. *Thunderstorm Source*

Thunderstorms are clustered in different types of weather systems under proper synoptic scale forcing. However, local thunderstorms can also develop under non-synoptic scale forcing environment when the static instability is enough to provide updrafts. In this situation, some meso-β scale and/or even meso-γ scale systems play an important role in convection initiation and development. These meso-scale systems usually form in the boundary layer.

During the mid-summer in the YRD controlled by a subtropical high, surface temperature gradient develops due to the radiation difference at different surface properties, such as the urban heat island and land-water borders. Roughness of topography or hills/mountains can generate convergence zones or upsloping updrafts. Therefore, thunderstorms are often triggered by low level updrafts associated with the low level meso-scale systems that are strongly correlated to the surface properties. By comparing the averaged distribution of thunderstorm with topographic factors for a long period, the effect of these factors on thunderstorm initiation development can be revealed.

For investigating the “source” of thunderstorm, the first two cells’ locations / footprints are selected for those thunderstorms with a *VILmax* at least 25 kg/m^2 and lifecycle duration at least 60 min in Fig. 10. Obviously, the first two cells (or “sources”) concentrate to smaller areas than all lifecycle cells shown in Fig. 5. Thunderstorm sources are highly correlated to some medium-sized cities (yellow circles in Fig. 9), such as Ningbo, Hangzhou, Shaoxing, Suzhou, Wuxi, and Changzhou. The urban heat island effect of the cities plays an important role in triggering convection. On the other hand, these cities are close to large water bodies, such as the Taihu Lake and the Hangzhou Bay, revealing that the temperature gradient along land-water border may intensify the local circulation with the UHI. Some other thunderstorm sources are located at some isolated mountains or hills (red circles in Fig. 9), such as the Siming Mountain, the Tianmu Mountain, and the Meishan Mountain. Raymond and Wilkening [1980] found large negative heat fluxes in the upper part of the convective core over the isolated mountains.

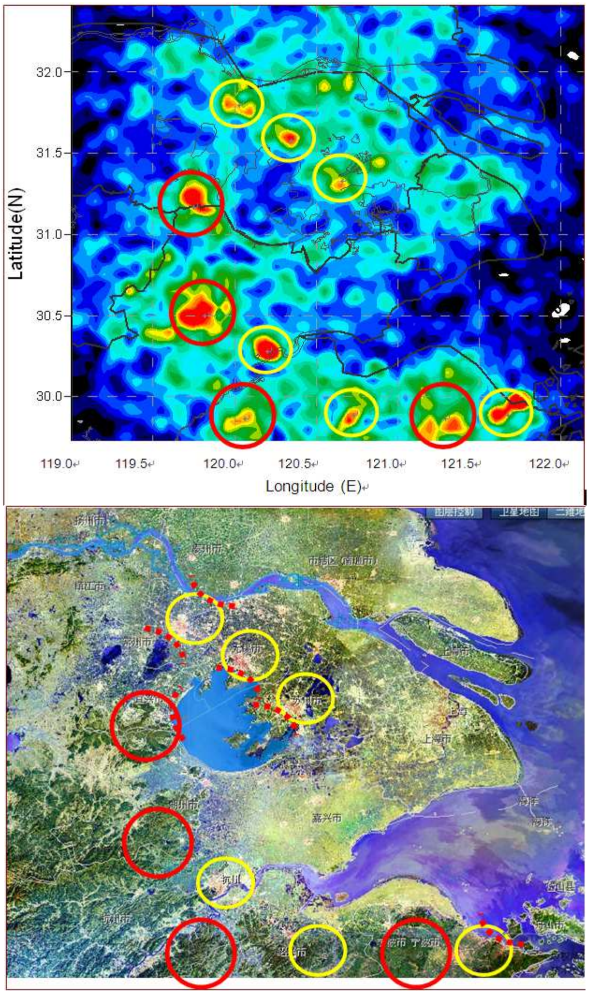

Fig. 9. Cell Density distribution of the first two cells of the thudnerstorms over the Yangtze Rive Delta (upper) and the Google Earth satellite topography image (lower). Red circles depict mountains, yellow for cities, and red dotted-curves for land-water borders.

B. Intensity Change of Thunderstorm

Using accumulated $\varDelta VIL_t$ (maximum VIL change between two radar scans), some intensity change centers are shown in Fig. 10 for local storms (upper) and medium-distance moving storms. Local thunderstorms tend to be slightly weakening over the urban areas of some medium-sized cities, while storm intensifying centers are found at about 10-30 km downwind of these city centers (Fig. 10 upper). The strengthening and weakening mechanisms relate to the underlying surface features. In the northern Baoshan District of Shanghai, a significantly thunderstorm intensifying area was found at the junction of the Yangtze River and the city. Along the Yangtze River, there are a series of harbors that may cause smaller heat islands to thunderstorm imitation, development, and maintenance. Therefore, more intensifying storms were found than weakening ones in this area. Similarly, thunderstorms tended to intensify in Ningbo Zhenhai and Beilun Port.

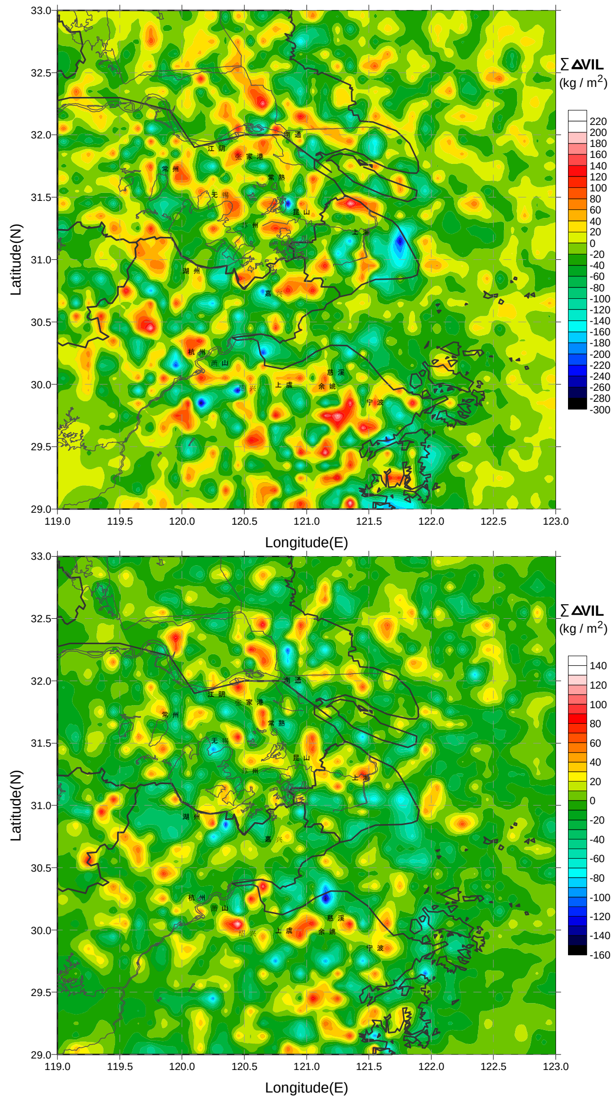

Fig. 10. Distribution of accumulated VIL change between two radar scans (in kg/m^2) of the thunderstorms with a life cycle at least 60 min, total path about 0-30 km (upper) and 30-60 km (lower), and the maximum VIL at least 25kg/m^2 during the months from April to September in 2004 to 2012 in the Yangtze River Delta.

Significantly, the intensifying area of the medium-distance moving storms also shows a downwind effect with a distance of 20-40km from medium-sized cities and centers of larger cities, while significant weakening areas are located over water body downwind of land (Fig. 10 lower). Long-distance moving thunderstorms usually intensified in two kinds of areas: in the land areas downwind of large water bodies, and over terrain with a windward slope (figures not given). Urban effect on precipitation and convection has been widely studied and similar results were found in other cities [Huff and Changnon, 1972; Changnon, 1976; Dixon and Mote, 2003; Chen et al. 2007] .

Fig. 11 compares the intensity change distribution of the local thunderstorms to the surface temperature gradient. Thunderstorms tend to intensify along the land-water border along the Yangtze River in the Baoshan District due to the sea-breeze front and the urban heat island from the urban areas of Shanghai south to Banshan. It is interesting that even though there is high surface temperature gradient and more local thunderstorms over the urban area of Shanghai (Fig. 6) than surrounding areas, fewer thunderstorms are intensifying here than Baoshan District. This reveals that sea-breeze front is more important than urban heat island effect for local thunderstorm in the intensifying phases (initiation and development) in Shanghai.

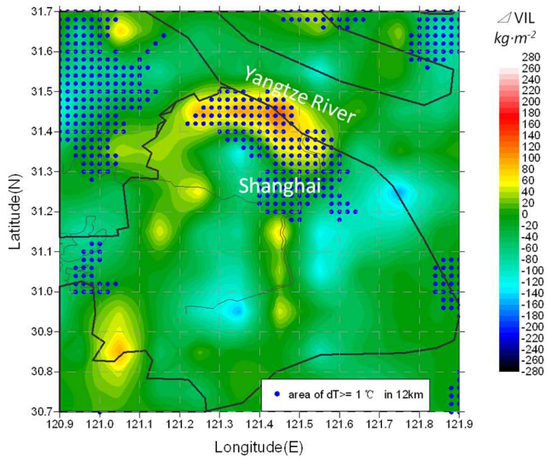

Fig. 11. Accumulation of $\varDelta VIL_t$ and zones with surface temperature gradient over 1 ºC /12 km (blue dots) at 12:00 BJT for Shanghai in July and August of the years from 2009 to 2012.

VI. TEMPORAL DISTRIBUTIONS OF THUNDERSTORMS

A. Diunral Characteristics of Thunderstorm Sturcture

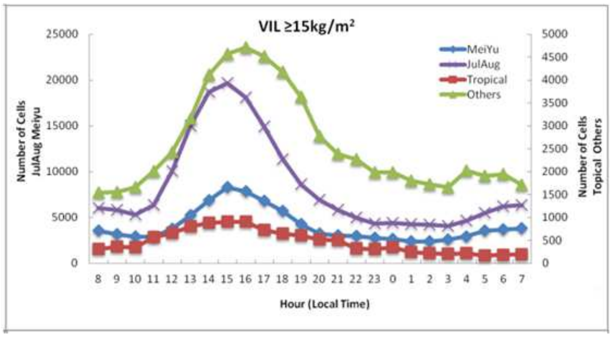

Fig. 12. Diurnal frequency distributions of storm cell (with a maximum VIL ⩾15kg/m^2) under four types of synoptic situation over the Yangtze River Delta region in the months of Apr. to Sep. during 2004 to 2012.

Fig. 12 shows the diurnal distributions of thunderstorm cell frequency in different synoptic types. Thunderstorms peak in the afternoon in midsummer and tropical systems, while they show a bimodal diurnal distribution during monsoon season and the others.

Midsummer thunderstorms with a *VILmax* of 15kg/m^2 (grade I) show the tallest and strongest vertical structure, followed by Meiyu season thunderstorms, and those with tropical weather systems the lowest, by comparing the echo top and the core height (the height of the cell maximum reflectivity -MRHGT) in Fig. 13. However, stronger thunderstorms (Grade II and Grade III) show less differences in storm structure among the various seasons (figures not given).

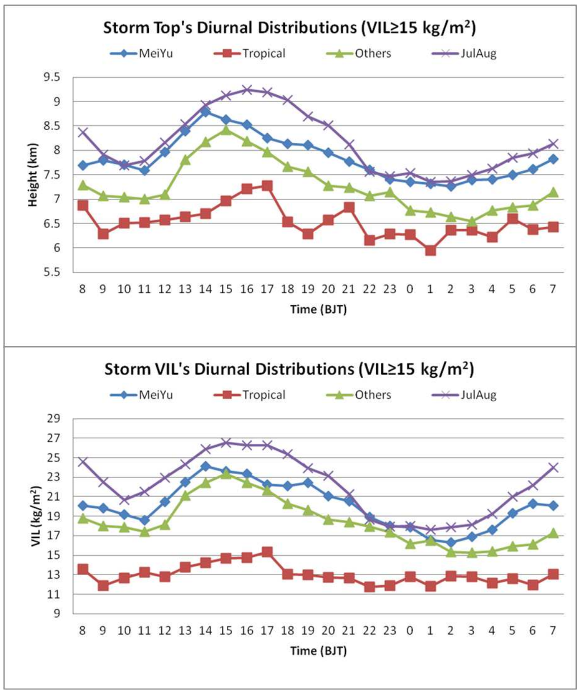

Fig. 13. Diurnal distributions of averaged (upper) storm top, and (lower) max reflectivity height (MRHGT) for cell with a maximum VIL ⩾15kg/m^2 under different synoptic conitditons over the Yangtze River Delta region 2004 to 2012.

B. Structure and Lightning Characteristics in Lifecycle

Thunderstorm evolution in its lifecycle has been studied using radar and lightning data [Toracinta et al., 1996; Chin and Wilhelmson, 1998; Wakimoto et al., 1998; Carey et al., 2003; Bunkers et al., 2006;]. Radar products and lightning products are compared in 6-min intervals during the life cycle. Fig. 14 shows some averaged structural parameters (such as VIL, ET, MRHGT, and height difference of base and maximum reflectivity -DBMR, etc.) and lightning flashes for the thunderstorms with *VILmax* at least 25kg/m^2 and lifecycle about 60 min. In the initiation stage of a thunderstorm, its core center is first observed in the mid-level. Then the top and core climb as the updraft intensifies, while the base descends as precipitation forms in the mid-level. When the thunderstorm develops to a certain extent, the core center cannot be lifted by the updrafts even if the updrafts are still strong. The core reaches its maximum height, while the top and base of the storm continue to rise and descend respectively. The strengthening of the updrafts also causes a burst of intra-cloud (IC) lightning activity and relatively small amounts of cloud-to-ground (CG) lightning. With the mass of hydrometeors (water droplets, hail, graupel, etc.) increasing, the core center begins a downward trend, but the storm top may still continue to raise with the upward motion and thunderstorm height increases. When the thunderstorm enters the outbreak stage, the IC lightning flash rate reaches its peak and the storm core center with big rain drops and hail balls declines rapidly. After that, updrafts weaken and downdrafts intensify, and IC lightning begin to weaken and CG lightning increases significantly since large amounts of charged water drops and hail descend. The decaying storm shows a fast descending top and core center very close to ground. CG flashes peak and a higher positive CG ratio follows. At last, the thunderstorm dissipates. Fig. 15 presents a basic conceptual model of thunderstorm evolution based on storm life cycle analyses above.

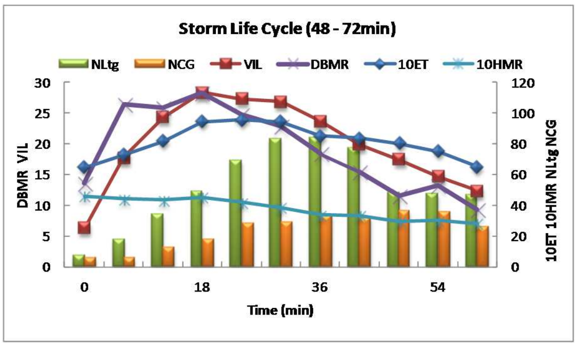

Fig. 14. Time series of some averaged structure parameters (ET, VIL,HMR.) and averaged total lightning flashes (NLtg) for the years of 2004-2008 and averaged cloud-to-ground lightning flashes (NCG) for the years of 2008-2012, for those thunderstorms (VIL⩾25kg/m^2) with a life cycle about 60 min.

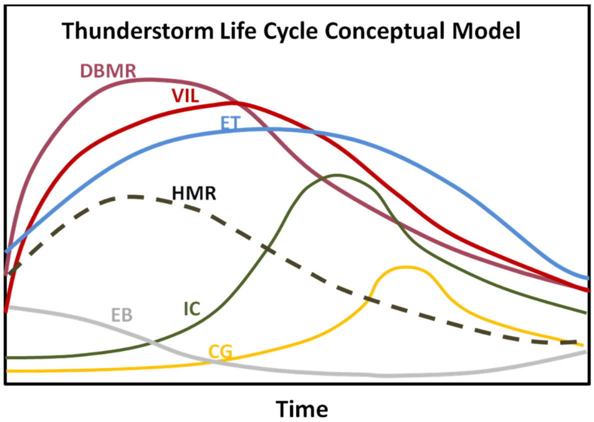

Fig. 15. Conceptual model of a thunderstorm's life cycle with the evolution of the echo top (ET), vertically integrated liquid (VIL), height difference of base and maximum reflectivity (DBMR), intra-cloud (IC) lightning flash rate, and cloud-to-ground (CG) lightning flash rate.

VII. CONCLUSIONS

Using the WSR-88D Doppler Weather radar and the Vaisala lightning detection data, some characteristics (the spatiotemporal distributions and motion features) of thunderstorms over the Yangtze River Delta (YRD) region are investigated. Vertical structure of storm cell and lightning activity during the evolutionary stages of several types of thunderstorms are also analyzed, and a basic conceptual model of thunderstorm evolution is built up.

In the YRD region, most of thunderstorms, especially those local storms, are close to some medium-sized cities, mountains or hills (especially those isolated), and water-land borders. This implies solar radiation and difference of underlying surface features are major causes of thunderstorms. The medium path thunderstorms tend to be close to the borders of land and water, while the long path thunderstorms concentrate in several major corridors under certain synoptic situations. Thunderstorms peak in the afternoon in midsummer while thunderstorms show a bimodal diurnal distribution during monsoon season. Midsummer thunderstorms show the tallest and strongest vertical structure, followed by Meiyu season thunderstorms, and those with tropical weather systems the lowest. However, severe thunderstorms show less difference among the various seasons. Local thunderstorms' initiation is often associated with an urban heat island, valley circulation, and land-water (sea or lake) circulation, mostly at 12-18 (LST) for the short- and medium-path thunderstorms.

Local storms tend to intensify and weaken in the same areas, such as cities, isolated mountains or hills, and water-land borders. Storm intensifying centers are found about 10-30 km downwind of the city centers. The strengthening and weakening mechanisms are related to the underlying surface features. Significantly, the strengthening area of medium-path storms also shows a downwind effect with a distance of 20-40km from medium-sized cities and centers of larger cities, while significant weakening areas are located over water body downwind of land. Long-path thunderstorms usually intensified in two kinds of areas: in the land areas downwind of large water bodies, and over terrain with a windward slope.

Evolutional characteristics in the lifecycle of different thunderstorms is analyzed using vertical structure of storm cell and lightning flashes, and a basic conceptual model of thunderstorm evolution is given.

REFERENCES

Ambum, S. A., and P. L., Wolf (1997), VIL density as a hail indicator. Wea. Forecasting, (12):73-478

Dai, J., H. Qin, and J. Zheng (2005), Analysis of lightning activity over the Yangtze River Delta using TRMM/LIS observations. Chinese J. Appl. Meteor. Sci. 16(6), 728-736 (in Chinese).

Carey, L. D., T. L. McCormick, M. J. Murphy, and N.W.S. Demetriades (2003), Three dimensional radar and total lightning structure of mesoscale convective systems. 31st Conf. on Radar Meteorology, Seattle, WA, Amer. Meteor. Soc., 80-83.

Changnon, S. A. (1976), Effects of urban areas and echo merging on radar echo behavior. J. Appl. Meteor., 15, 561–570

Chen, T. C., S. Y. Wang, and Yen M. C. (2007), Enhancement of afternoon thunderstorm activity by urbanization in a valley: Taipei. J. Appl. Meteor., 46:1324-1340

Dixon, P. G. and T. L. Mote (2003), Patterns and causes of Atlanta's urban heat island–initiated precipitation. J. Appl. Meteor., 42, 1273–1284

Fuquay, D. M. (1982), Positive cloud-to-ground lightning in summer thunderstorms, J. Geophys. Res., 87, 7131-7140.

Greene, D. R. and R. A. Clark (1972), Vertically integrated liquid water-a new analysis tool, Mon. Wea. Rev., 100, 548-552.

Huff, F. A. and S. A. Changnon (1972), Climatological assessment of urban effects on precipitation at St Louis. J. Appl. Meteor. 11: 823-842.

Johnson, J. T., P. L. MacKeen, A. Witt, et al. (1998), The Storm Cell Identification and Tracking (SCIT) algorithm: An enhanced WSR-88D algorithm. Wea. Forecasting, 13, 263-276.

Macgorman, D. R., and D. W. Burgess (1994), Positive Cloud-to-Ground Lightning in Tornadic Storms and Hailstorms. Mon. Wea. Rev., 122, 1671–1697.

Raymond, D. and M. Wilkening (1980), Mountain-Induced Convection under Fair Weather Conditions, J. Atmos. Sci., 37, 2693–2706.

Reap, R. M., and D. R. MacGorman (1989), Cloud-to-Ground Lightning: Climatological Characteristics and Relationships to Model Fields, Radar Observations, and Severe Local Storms. Mon. Wea. Rev., 117, 518–535

Sanders, F. (1999), A proposed method of surface map analysis. Mon. Wea. Rev., 127, 945–955.

Shu, J., T. Jiang, and X. Yang (2000), Characteristic analysis of the Shanghai Urban Heat Island effec, Shanghai Environmental Secience, 19, 532-534

Toracinta, E. R., K. I. Mohr, E. J. Zipser, and R. E. Orville (1996), A comparison of WSR-88D reflectivities, SSM/I brightness temperatures, and lightning for mesoscale convective systems in Texas. Part I: Radar reflectivity and lightning. J. Appl. Meteor., 35, 902–918.

Wakimoto, R. M., C. Liu, and H. Cai (1998), The Garden City, Kansas, Storm during VORTEX 95. Part I: Overview of the Storm's Life Cycle and Mesocyclogenesis. Mon. Wea. Rev., 126, 372–392

Williams, E. R., B. Boldi, A. Matlin, M. Weber, S. Hodanish, D. Sharp, S. Goodman, R. Raghavan, and D. Buechler (1999), The behavior of total lightning activity in severe Florida thunderstorms. Atmos. Res., 51, 245-265.

Zhang K, Wang R, Shan C, Da L. (2009), Temporal and spatial characteristics of the urban heat island during rapid urbanization in Shanghai, China. Environmental Monitoring and Assessment. 169(1-4):101-112.